MAE 298 Aeroacoustics – Final Project
Review of Techniques for Predicting Aeroacoustics of Aerospace Vehicles During Launch, Ascent, and Abort

Logan D. Halstrom

Graduate Student

Department of Mechanical and Aerospace Engineering

University of California, Davis, CA 95616

I. Introduction

Define launch vs ascent vs abort
History of aeroacoustic testing in aerospace vehicles.[5]
analytic modeling for propulsion acoustics.[2]

II. Experimental Methods

One of the most straight forward methods of predicting aeroacoustic vibrational effects on aerospace vehicles is through full-scale testing of sections or complete models of the flight vehicle. A very detailed summary of design methodologies governing these kinds of test can be found in Himelblau et al. (1970),[5] which will be summarized in the following sections.

The paper specifically addresses the effectiveness of vibrational testing versus acoustic testing of aerospace vehicles. Vibrational testing facilities utilize electromagnetic or hydraulic shakers to apply vibrational loads to test articles. Alternatively, acoustic testing involves placing the test article within an acoustic field, similar to that of the flight condition. At the time of publishing (1970) acoustic testing was relatively new, with its first major usage during the testing of the Titan missile. Some methods of acoustic testing will now be detailed.

II.A. Ground Testing

The most straight-forward of testing methods described by Himelblau is the free-field test, where the test article is subjected to an outdoor, unconstrained aeroacoustic field produced by some source, an example of which is shown in Fig 1. The acoustic source in this example is the exhaust of a blowdown wind tunnel, where a fluid upstream of the wind tunnel is pressurized and then released at supersonic speeds through the test section.[7] This high pressure fluid then exits the wind tunnel at high speeds, creating conditions similar to that of ascent.

In addition to supersonic wind tunnels, static-fire rocket engine tests can also be used as an acoustic source. Thus, in the early days of aeroacoustic testing, test could be performed for reduced cost by "free-riding" an already existing wind tunnel or rocket engine test.

Acoustic tests can also be performed in more contained facilities. One example is a reverberant test facility, which is a large chamber surrounded by noise-producing horns.[8] These horns allow the production of acoustic vibrations similar to the flight conditions to which sections of the test vehicle can be subjected.

Another method of testing, which was utilized in the ascent certification of the Apollo program lunar and command modules, is the progressive wave facility. This facility is a chamber with a large number of ducts connecting the test chamber to the outside of the structure, which is excited by an acoustic source (See Fig 2). The ducts are independently operable to allow control of the acoustic conditions inside the test chamber.[12] This method combines the realistic acoustic source advantages of the free-field test method with some level of source control as found in the reverberant chamber method.

Himelblau demonstrates that these aforementioned acoustic testing methods are superior to traditional vibrational testing methods due to a number of factors:

1. Vibration spectra that are more similar to flight conditions

2. Test article is not constrained at vibration force application points

3. Ability to test large structural article allows more similar modal characteristics to flight

However, he also states that there are still some limitations when it comes to acoustic testing. First, it can be difficult to select the proper vibration spectrum for flight condition matching, especially when the acoustic source is a "free-ride" wind tunnel or rocket engine test that is not specifically designed for the acoustic experiment. Additionally, free-field and progressive wave tests may be sufficient in the longitudinal direction parallel to the flow direction, but may not achieve the correct flow characteristics in the circumferential direction perpendicular to the flow. Finally, the propagation speed of the acoustic test are most likely not identical to that of the flight condition.

For these reasons, it is usually necessary to perform a full-scale flight test as the final certification, which Himelblau details and which is summarized in the next section.

II.B. Flight Testing

A full-scale test flight of an aerospace vehicle is a very expensive operation. For this reason, Himelblau states that it is highly important to have sufficient instrumentation onboard in order to clearly determine the cause and location of a failure if one occurs. This is vital in minimizing redesign costs in the case of a failure.

Himelblau reveals that calculations of aeroacoustic effects on structural integrity require a vast amount of data sampling, which was especially constraining in 1970 with limited bandwidth telemetry computers. For modern tests, the transmission limitation is somewhat alleviated by modern computers, but there is still the additional consideration that many different tests will be running simultaneously during the test flight (e.g. structural, aerodynamic, etc.), and sensor bandwidth must be budgeted between all of these.

II.C. Microphone Phased-Array

A more modern approach to flight test measurements is detailed in the paper by Panda et al. (2013),[9] which describes how a microphone phased-array (MPA) can be used to observe launch aeroacoustic conditions accurately from a distance, an example of which is shown in Fig 4. A MPA is a device that consists of many microphones spread out over some area (e.g. 70 microphones on a 10ft x 10ft area). The multiplicity of the microphones allows the device to sense not only noise source strength but also location, which is vastly superior functionality to that of traditional single-microphone sensors.

For the test described by Panda, the MPA was designed to maximize lower frequency resolution while adhering to manufacturability constraints. Microphones were constrained from being to close to one another and also could not occupy the center where a camera was located. Adhering to these constraints, sensors were placed in logarithmic spirals traveling outward from a center ellipse, and the empty corners were filled in with additional sensors. The MPA was mounted to a lift about 400 ft away from the rocket, which was raised 40ft in the air and secured by guy wires to prevent motion of the MPA during launch.

During the static fire and actual launch of the Anteres rocket, the MPA was able to determine very specific information about the acoustic sources, greatest of interest being the dominant noise sources. It was found that during the static fire, the duct exit was the primary noise source, not the duct exit plume as suggested by previous models. During launch, the dominant source varied with

time, starting with the duct exit, but transitioning to the top of the launch pad as the rocket rotated to avoid the service mast.

Specific source information such as the data produced in this experiment can be extremely useful in determining design improvements that will minimize aeroacoustic effects.

III. Wind Tunnel Testing

Aside from full-scale testing, another method for creating flight-like aeroacoustic conditions is through sub-scale wind tunnel testing. Modern machining techniques (e.g. laser drilling, additive manufacturing, etc.)[3] allow production of orders of magnitude higher fidelity models than in the past. Fine accuracy modeling of vehicle geometry details is extremely important in recovering the specific aeroacoustic environments that are to be expected on the flight vehicle.

To illustrate modern wind tunnel testing methods for aerospace vehicles, we will look at to analyses for NASA's Space Launch System (SLS) rocket. The first, Herron et al. 2016,[3] concerns ascent aeroacoustics during transonic flight. The second, Panda et al. 2011,[10] simulates the abort condition, where plumes from the abort rocket motors envelope the vehicle structure, creating additional acoustic effects.

III.A. Ascent Wind Tunnel Testing

For ascent testing of SLS, extremely high fidelity 2.5% and 4% models of the rocket were manufactured. The models could be reconfigured to represent various launch configurations. The extra-fine geometry details of the model can be admired in Fig 5.

To measure unsteady aeroacoustical pressure fluctuations, the models were instrumented with over one hundred unsteady pressure transducers, placed according to the locations demonstrated in Fig 6. Following best practices, the sensors were placed in holders that were individually contoured to be flush with the model, minimizing the broadband noise induced by surface irregularities. Additionally, the models were fitted with static pressure taps to provide surface pressure readings for CFD model comparison and validation.

Tests were conducted in the NASA Ames Unitary Wind Tunnel and Supersonic Wind Tunnel at Mach numbers ranging from 0.7 to 2.5. Aside from pressure transducer readings, the wind tunnel tests were also able to produce visual flow information in the form of the shadowgraphs shown in Fig 7. During the tests, the model was dynamically pitched to produce rate-dependent aeroacoustic results.

The data produced in this testing campaign were used to supply the design databases for SLS as well as analysis of venting environments and validation of unsteady CFD simulations. This extremely detailed information is invaluable in aerodynamic design and cannot be produced using the experimental method described in previous sections.

III.B. Abort Wind Tunnel Testing

During crewed launches of SLS, the crew module will be capable of abort separation during the event of a rocket failure. This process involves a tractor rocket motor call the Launch Abort System (LAS) that pulls the crew capsule away from the main rocket in the direction of the rocket's motion. Because the rocket motor is located upstream of the vehicle structure, the unsteady plumes of the

rockets will interact directly with the structure as well as with the surrounding flow and shocks, creating additional aeroacoustic effects that are extremely difficult to model.

Testing the effect of live solid rocket motors in a wind tunnel can be very expensive. For this reason, Panda instead chose to add taps to the 6% Orion model (see Fig 8) which would supply heated Helium gas to the model rocket nozzles in the LAS. In general, the molecular properties of Helium are very different than those of solid rocket motor exhaust compositions. However, looking at the Lighthill stress tensor (Eqn 1), which is considered to be the primary contributer to aeroacoustic noise in this type of flow, we can see that the noise source is dependent on changes in ρuu, which depends on local dynamic pressure, and changes in $p - c^2\rho$, which corresponds to entropy fluctuations. These two expressions are not entirely dependent on the chemical nature of the fluid and thus, high-pressure Helium heated to 700^oF can be made to behave like solid rocket exhaust (acoustically, at least).

$$\overline{T}_{ij} = \rho u_i u_j + \delta_{ij}\left(p - c^2\rho\right) \tag{1}$$

There are some inconsistencies with this technique that cannot be avoided, which must be considered as a caveat when utilizing the test data. Specific insufficiencies in heated Helium as a replacement of rocket exhaust are:

1. No after-burning of unburnt fuel
2. No particle-damping
3. Incorrect specific heat ratio

Despite these deviations, it is assumed that Helium will otherwise behave sufficiently as an exhaust plume substitute.

Tests were conducted in the Unitary Wind Tunnel at NASA Ames at Mach numbers ranging from 0.3 to 1.2. Shadowgraph images were taken to visualize the flow and an infra-red camera was used to map model surface temperatures. To measure pressure fluctuations during the wind tunnel test, the model was fitted with 237 pressure transducers similar to those used in the previously described wind tunnel test.

Test results yielded extremely complicated flow fields, as demonstrated in the shadowgraph image in Fig 9. In the image, it can be seen that the plumes are focused and small in diameter for lower ambient flow Mach numbers, but very much expanded in size at higher Mach numbers. This expansion causes a much larger vehicle surface area envelopment by the plumes. However, pressure transducer data demonstrated that the smaller, more focused plumes generated more powerful aeroacoustic effects due to the plume edge shear layers compared to their less coherent, high-Mach counterparts.

Transducer readings were also scaled up to compare to a full-scale launchpad abort test and showed reasonable comparison, when considering the hot Helium caveats previously mentioned.

Overall, this test demonstrates that masterful manufacturing and clever, high-tech instrumentation can achieve highly complex experiments that produce detailed and useful aeroacoustic results.

IV. Computational Methods

Finally, the latest advent in the field of aerodynamics and aeroacoustics has been the usage of computers to simulate unsteady flows over aerospace vehicle geometries through computational

techniques like Computational Fluid Dynamics (CFD) and Computational Aero-Acoustics (CAA). These new developments are an exciting trend, because they allow the simulation of many more flight conditions and configurations at a marginal cost in comparison to the wind tunnel and flight testing examples that have been previously discussed. This cost savings comes with the price of error and inaccuracy due to approximate methods, but the field is ever-improving and even now can produce useful results for the correct applications.

Though modern CFD currently lacks the ability to resolve many unsteady, fluctuating flow features due to lower-order numerical schemes and reflective boundary conditions, useful information about the flow fields defining the aeroacoustic problem can still be derived using these techniques. In this section, a CFD simulation of the same Launch Abort System (LAS) analyzed in the previous wind tunnel test will be summarized and then a CAA code that could be used to further pursue aeroacoustical analysis will be discussed.

IV.A. Computational Fluid Dynamics

The paper by Childs et al. 2011[1] demonstrates CFD modeling of the same abort conditions simulated in the previous wind tunnel test. Simulations were performed using the NASA OVERFLOW CFD tool and grids were constructed using the overset Chimera Grid Tools. The advantage of using overset grids in this case is that it is relatively easy to construct complex and fine geometries such as the abort motors in Fig 10 compared to unstructured grids. As detailed in the ascent wind tunnel test section, the fine-scale geometries are critical for resolving the specific aeroacoustic effects.

The simulation of rocket plumes in Overflow is as simple as creating the correct boundary conditions inside of the rocket nozzle geometry (which slightly less extravagant than super-heating Helium gas). After considerable convergence testing to optimize choices of grid spacing, time-accurate settings, and turbulence models, a campaign of test conditions were simulated, producing results like those depicted in Fig 11.

These results are similar to those produced by the corresponding wind tunnel test, but now the surface pressure data is available for the entire surface geometry and flow field, which is a very powerful asset to have when analyzing problems such as LAS dynamic stability. Comparison to the wind tunnel test can be further supported by comparing plume shadowgraph images, like Fig 12.

Still, the caveat to this analysis is that the CFD cannot resolve the unsteady pressure fluctuations created by aeroacoustic noise. In this aspect, the wind tunnel test is superior. However, aeroacoustic effects may not always be out of reach of computational methods, as will be discussed in the next section.

IV.B. Computational Aeroacoustic Analysis

V. Conclusions

References

[1]Childs, R. E., Garcia, J. A., Melton, J. E., Rogers, S. E., Shestopalov, A. J., and Vicker, D. J., "Overflow Simulation Guidelines for Orion Launch Abort Vehicle Aerodynamic Analyses", in *29th AIAA Applied Aerodynamics Conference*, Submitted, 2011.

[2]Eldred, K. M. and Jones, G. W., Jr., "Acoustic load generated by the propulsion system", NASA SP-8072, 1971.

[3]Herron, A. J., Crosby, W. A., and Reed, D. K., "Overview of the Space Launch System Ascent Aeroacoustic Environment Test Program", in *54th AIAA Aerospace Sciences Meeting*, Submitted, 2016.

[4]Hill, R. E., and Coody, M. C., "Vibration and Acoustic Environments for Payload/Cargo Integration", AIAA paper 83-0329, Jan 1983.

[5]Himelblau, H., Fuller, C. M., and Scharton, T. D., "Assessment of Space Vehicle Aeroacoustic-Vibration Prediction, Design and Testing", NASA CR-1596, July 1970.

[6]Kiris, C. C., Barad, M. F., Housman, J. A., Sozer, E., Brehm, B., and Moini-Yekta, S., "The LAVA Computational Fluid Dynamics Solver", in *52nd AIAA Aerospace Sciences Meeting*, Submitted, 2014.

[7]Lockheed Martin, "High Speed Wind Tunnel and Test Systems Design Handbook", Publication Number AER-EIR-13552-E, 2002.

[8]Murray, F.M., "Operational Characteristics of a 100,000-Cubic-Foot Acoustic Reverberant Chamber", *The Shock and Vibration Bull.* No. 37, P. 5, Jan. 1968, pp. 13-24.

[9]Panda, J., Mosher, R. N., and Porter, B. J., "Identification of Noise Sources During Rocket Engine Test Firings and a Rocket Launch Using a Microphone Phased Array", NASA TM-2013-216625, Dec 2013.

[10]Panda, J., James, G. H., Burnside, N. J., Fong, R. K., Fogt, V. A., and Ross, J. C., "Use of Heated Helium to Measure Surface Pressure Fluctuations on the Launch Abort Vehicle During Abort Motor Firing", AIAA paper 2011-2901.

[11]Vicker, D. J., Childs, R. E., Rogers, S. E., McMullen, M. S., Garcia, J. A., and Greathouse, J. S., "Effects of the Orion Launch Abort Vehicle Plumes on Aerodynamics and Controllability", in *51st AIAA Aerospace Sciences Meeting*, Submitted, 2013.

[12]Wren, R.J., Dorland, W.D., and Eldred, K.M., "Concept, Design and Performance of the Spacecraft Acoustic Laboratory", *The Shock and Vibration Bull.* No. 37, P. 5, Jan. 1968, pp. 25-54.

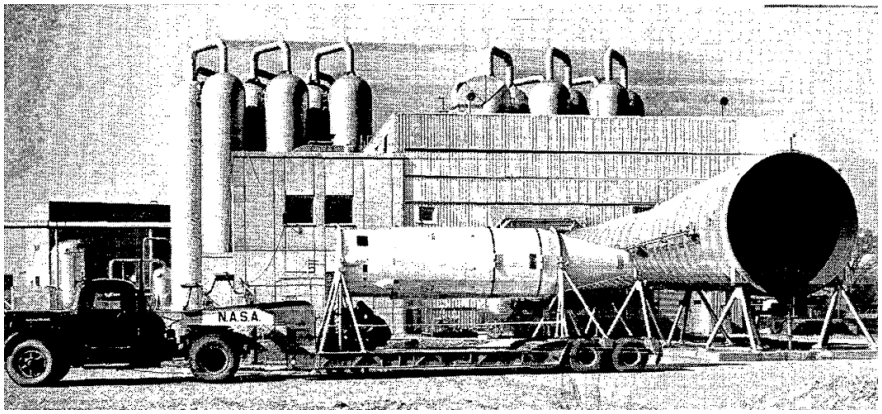

Figure 1: Acoustic test of the OGO spacecraft near the discharge nozzle of a large blowdown wind tunnel[5]

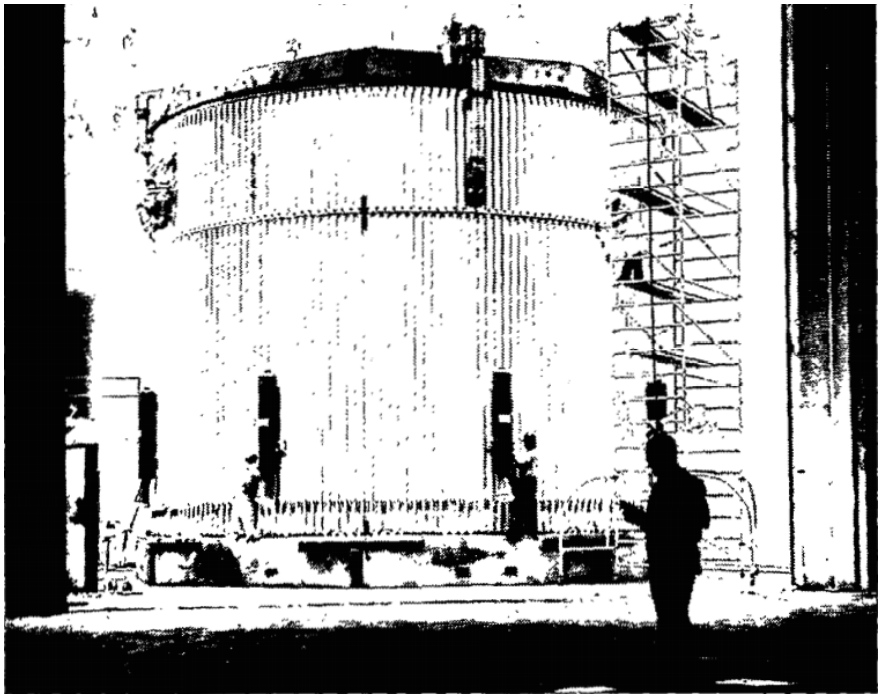

Figure 2: A Laboratory acoustic test of the thrust structure, aft skirt, and interstage of the S-II stage, Saturn V launch vehicle in a reverberant test facility[5]

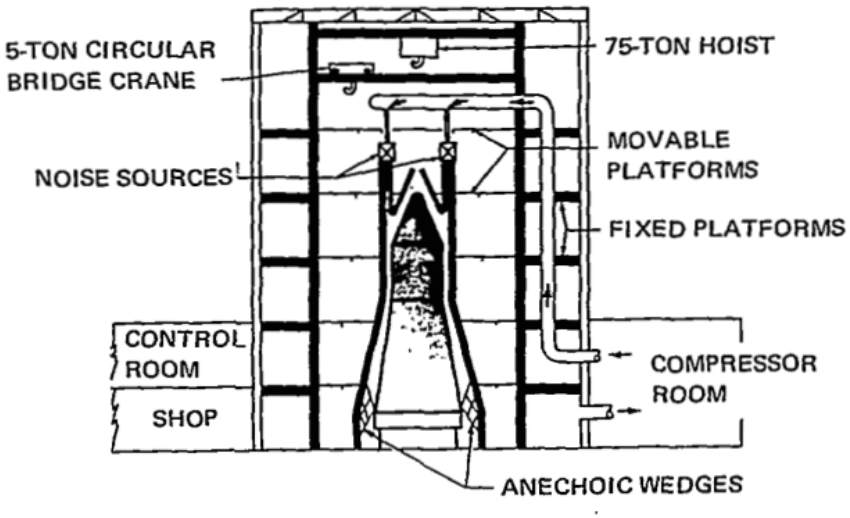

Figure 3: Laboratory acoustic test of the Apollo spacecraft in a progressive test facility[5]

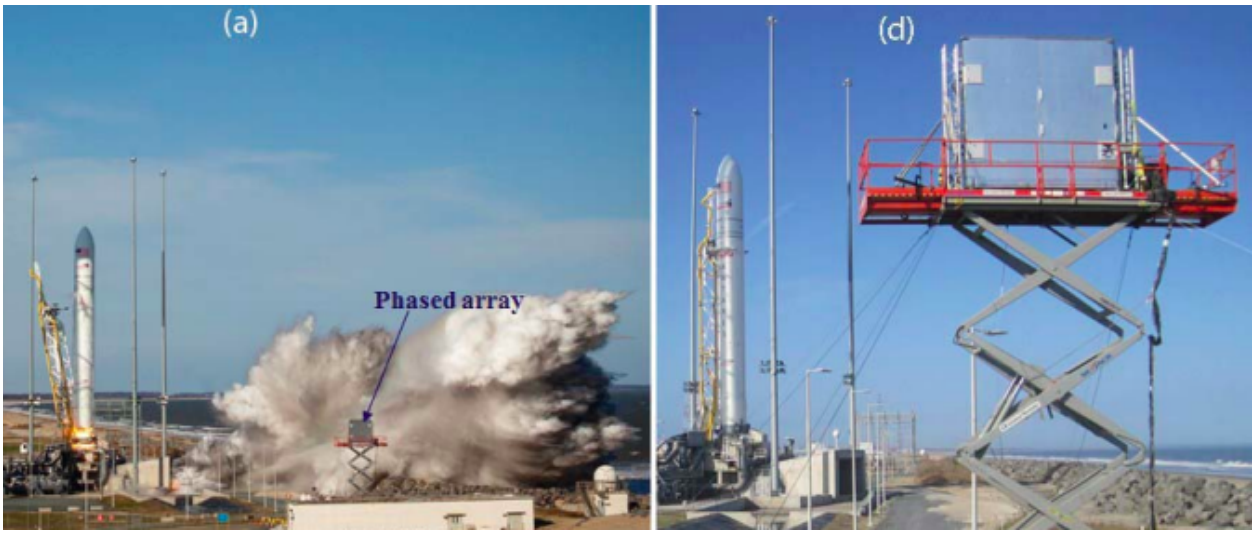

Figure 4: A microphone phased-array observing an Antares rocket launch[9]

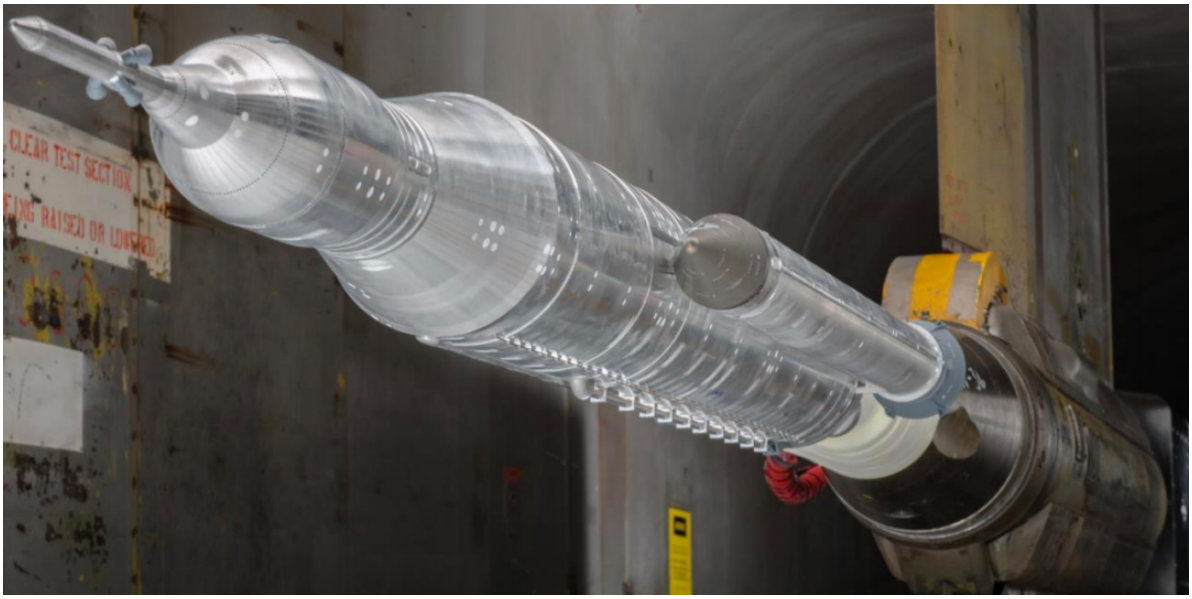
Figure 5: SLS 2.5% scale wind tunnel model[3]

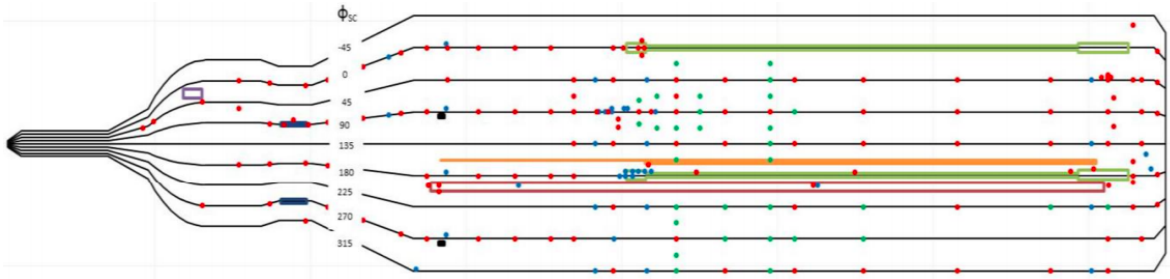

Figure 6: SLS 2.5% scale wind tunnel model sensor locations[3]

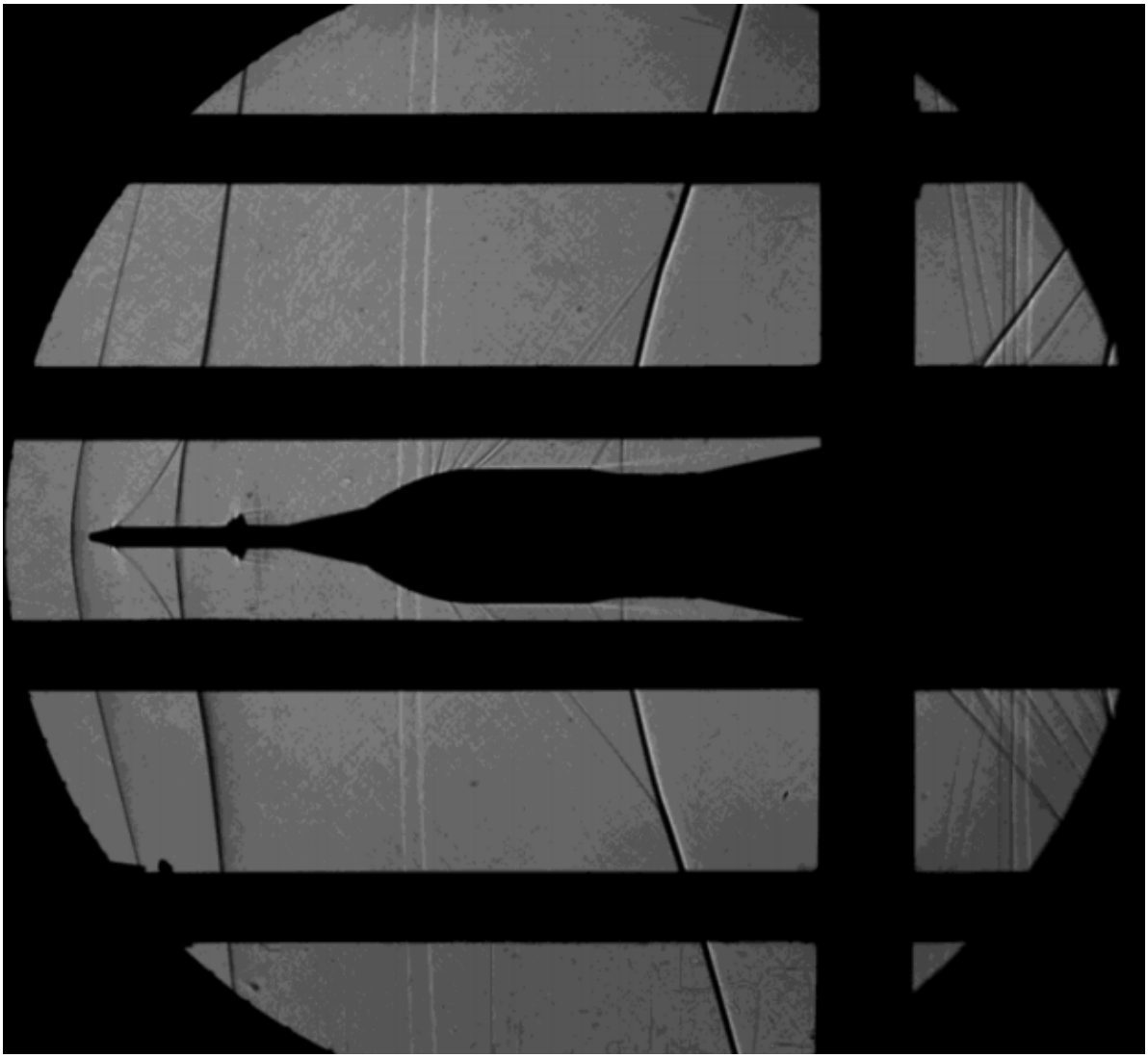

Figure 7: SLS 2.5% scale wind tunnel shadowgraph during transonic flight[3]

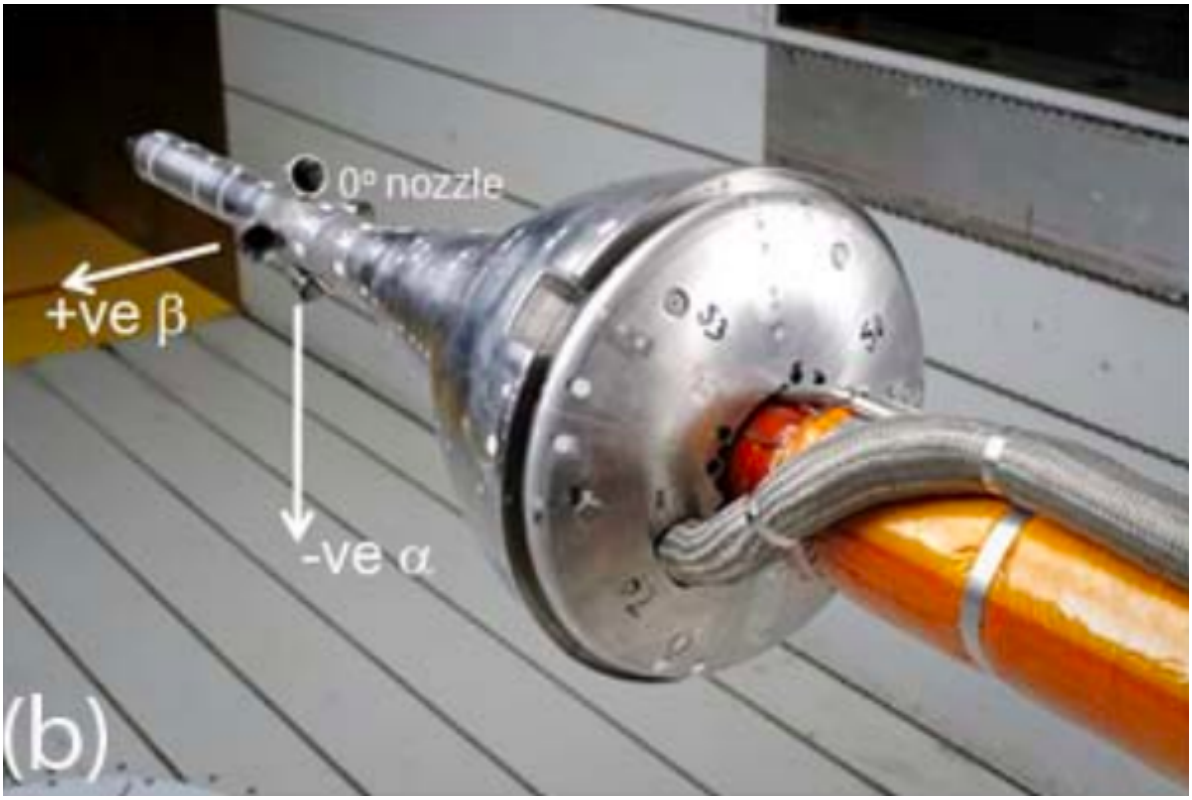

Figure 8: Orion Launch Abort System sub-scale wind tunnel model with hot helium taps for exhaust plume simulation[10]

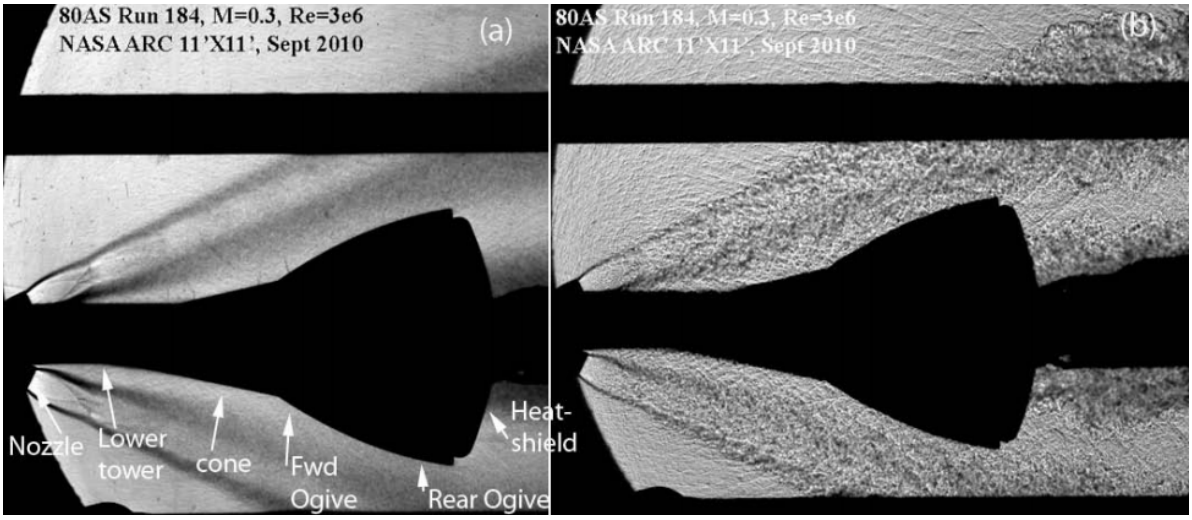

Figure 9: Orion Launch Abort System sub-scale model shadowgraph with hot helium plumes creating unsteady effects[10]

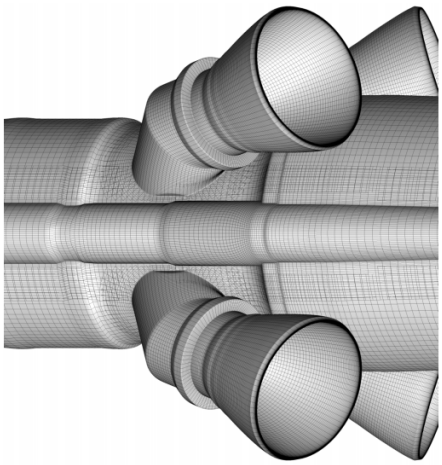

Figure 10: Orion Launch Abort System CFD grid showing fine geometry features[11]

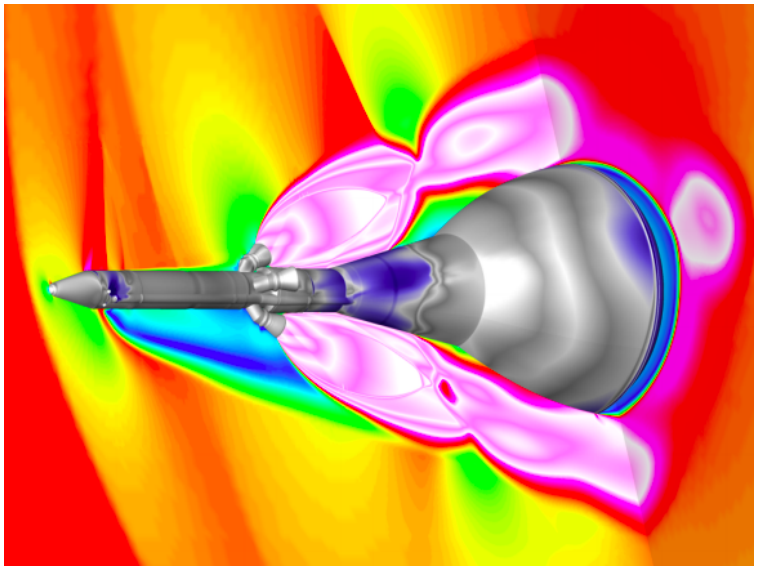

Figure 11: Orion Launch Abort System CFD modeling of plume impingement[11]

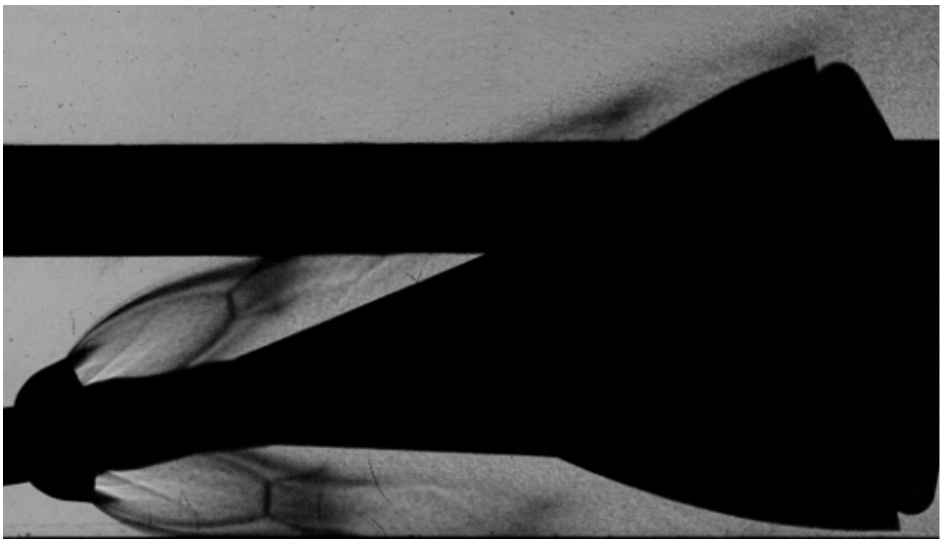

Figure 12: Orion Launch Abort System CFD shadowgraph that is remarkably comparable to the corresponding wind tunnel test[1]